ORGANIC PROCESS RESEARCH & DEVELOPMENT
OPR&D

Communication

An Alternative Indazole Synthesis for Merestinib

Yu Lu, Kevin Paul Cole, Jared Fennell, Todd Maloney,
David Mitchell, Ramesh Subbiah, and Balakumar Ramadas

Org. Process Res. Dev., **Just Accepted Manuscript** • DOI: 10.1021/acs.oprd.8b00016 • Publication Date (Web): 21 Feb 2018

Just Accepted

ACS Publications

Organic Process Research & Development is published by the American Chemical Society. 1155 Sixteenth Street N.W., Washington, DC 20036

An Alternative Indazole Synthesis for Merestinib

Yu Lu, Kevin P. Cole, Jared W. Fennell, Todd D. Maloney, [†]David Mitchell, [§]Ramesh Subbiah, and [§]Balakumar Ramadas*

Small Molecule Design and Development, Lilly Research Laboratories, Eli Lilly and Company, Indianapolis, Indiana 46285

[§]Syngene International Ltd., Biocon Park, Plot No. 2 & 3, Bommasandra IV Phase, Jigani Link Road, Bangalore 560 099, India

Table of Contents Graphic

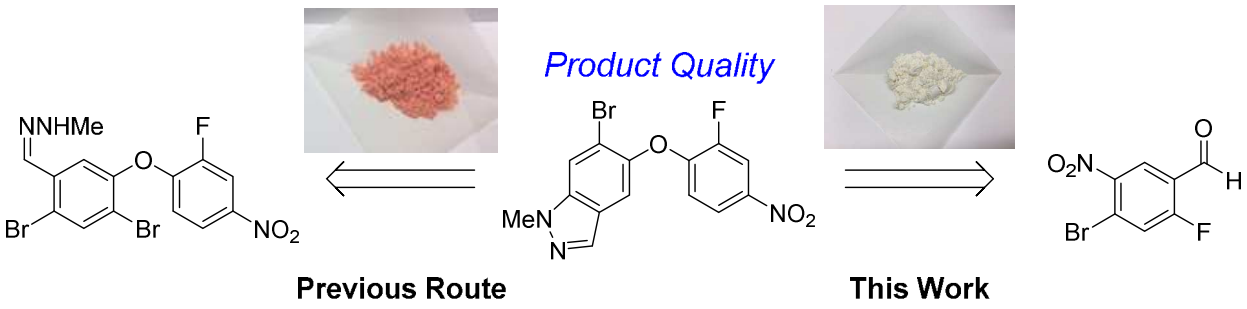

ABSTRACT. A new synthesis of a key indazole-containing building block for the MET kinase inhibitor merestinib was designed and demonstrated. Crucial to the successful construction of the challenging indazole is an S_NAr reaction, which forges the heterocyclic ring. Continuous processing was applied to two of the five steps: nitration of a benzaldehyde and high temperature hydrolysis of an aniline to phenol. When compared to a highly-developed historical route, the new route shows clear benefit in terms of product quality and potentially manufacturability and robustness.

Keywords: merestinib, indazole, nitration, S_NAr, continuous flow, thermohydrolysis

INTRODUCTION

Merestinib (Figure 1, **1**) is a MET inhibitor[1] currently in clinical trials as therapy for a number of oncolytic indications.[2] Marketed MET inhibitors include crizotinib (Xalkori®)[3] and cabozantinib (Carbometyx®).[4] They were the first MET inhibitors approved by the U.S. Food and Drug Administration (FDA). Crizotinib was approved in 2011 to treat late-stage non-small cell lung (NSCL) cancers. Also, in 2011, carbozantinib was approved by the FDA as an orphan drug to treat medullary thyroid cancer. Both MET inhibitors are currently being evaluated for other types of cancers.[5]

The current synthesis approach for **1** involved a convergent approach in which three fragments (**2**, **3**, and **4**) are united. The pieces can be assembled using Suzuki cross-coupling, nitro group reduction, amide bond formation, and unmasking of the pyrazole moiety; thus far in development two different step orderings have been employed for API manufacturing. Indazole fragment **2** has been a constant intermediate, and has served as a key building block.[6] The complexity of **2** presents several daunting synthetic challenges: the 5,6-substitution pattern of the methylindazole ring (which can also be viewed as a tetrasubstituted benzene derivative), electronic activation requirements for indazole formation, and the *N*-methyl substitution of the heterocycle which introduces the possibility of N1 vs. N2 regioisomerism in any methylation approach.

Figure 1. Retrosynthesis of Merestinib

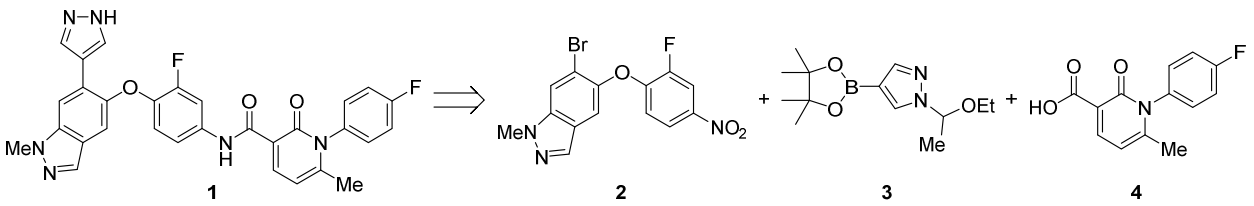

A number of synthesis routes have been evaluated for the preparation of **2**. Prior to this work, the most recently developed approach involved a four step transformation utilizing Cu-catalyzed cyclization of a methyl hydrazone to form the indazole ring (Scheme 1).[7] The substitution pattern is first set by selective dibromination of 3-hydroxybenzaldehyde (**5**). Phenol **6** was reacted with 1,2-difluoro-4-nitrobenzene **7** in an S_NAr reaction to form diaryl ether **8**. Hydrazone **9** was then obtained by reacting aldehyde **8** with aqueous methylhydrazine. Indazole formation finally provides **2** by means of an intramolecular Cu-catalyzed Ullmann-like ring closure between the hydrazone and aryl bromide.[8]

Scheme 1. Previous Synthesis of Indazole 2

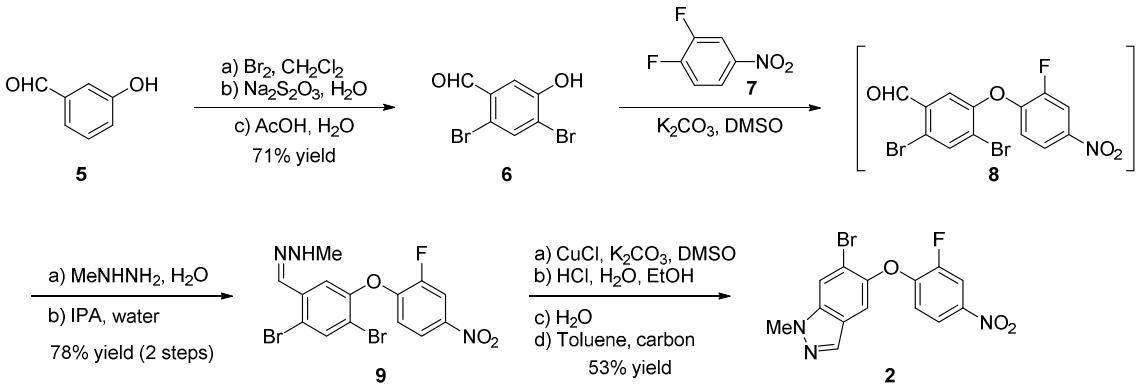

On multi-kilogram scale, the first three steps have proven robust and typically provide 50–55% yield across the sequence. However, even after several rounds of development, the Cu-catalyzed step continues to present challenges at plant scale. Specific problems with this synthetic route in the pilot plant were: 1) Use of dichloromethane and bromine for the

bromination step proved optimal for reactivity and regioselectivity. For environmental reasons, dichloromethane is considered highly undesirable at Eli Lilly for long term manufacturing use. 2) For the Ullmann indazole ring closure, a rigorously oxygen-free atmosphere was necessary to avoid low product recovery. Despite our best efforts this step still proved to exhibit substantial variability in terms of performance, impurity profile, product quality, and yield (37–57%). 3) For the Ullmann indazole ring closure, long cycle time during the extensive purification process limited throughput. The purification consisted of a technical grade crystallization, carbon treatment, and recrystallization in order to ensure acceptable quality of indazole **2** in terms of residual copper content, product color, and overall impurity load. Notably, as shown in Figure 2, at least 50 discrete impurities are formed during the Cu-catalyzed indazole ring formation! In parallel with further attempts at development of the existing route, these findings caused us to revisit the route selection strategy for a possible alternative approach to **2**.

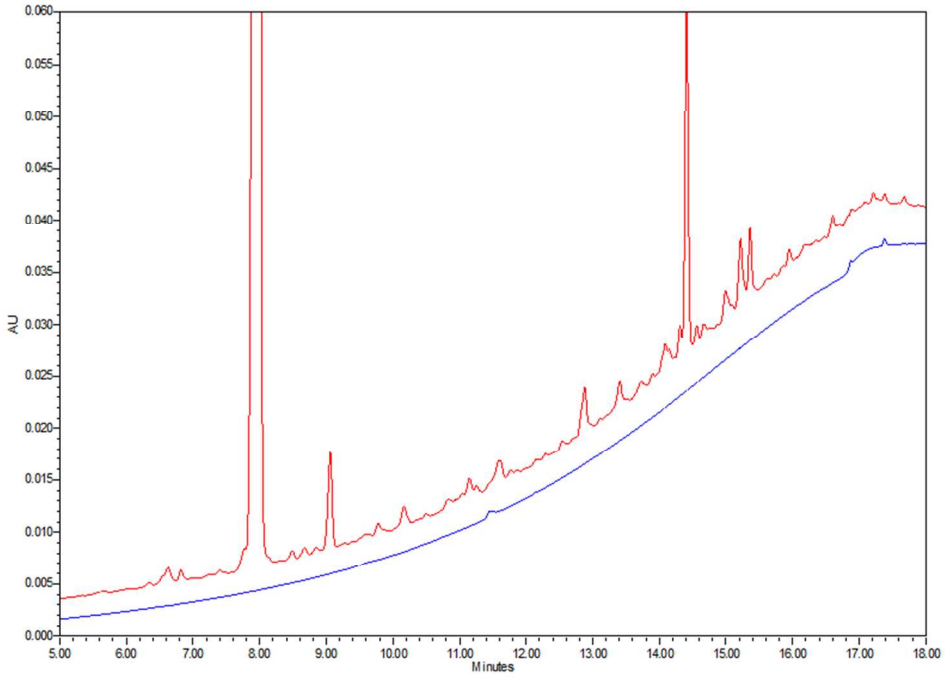

Figure 2. HPLC chromatogram (240 nm) of solid **2** after initial isolation (red trace, top) compared to blank injection (blue trace, bottom). In this chromatogram, **2** elutes at ~8 min, but

at least 50 peaks can be integrated, and the main peak has an approximate area percentage of 88.3%.

RESULTS AND DISCUSSION

1. Route Design and Selection. Since we chose to revisit the route selection approach for **2**, the data from previously investigated routes was re-evaluated. A summary of the route design is presented in Scheme 2. In addition to the copper-enabled synthesis route (Scheme 2, Equation 1), there were three main additional approaches considered. The key transformation in each approach are as follows: Equation 2: selective bromination of a preformed indazole ring; Equation 3: An S_NAr approach to the indazole using an electronically unactivated substrate; and Equation 4: An intentionally activated substrate for S_NAr formation of the indazole.

Scheme 2. Route Design Summary

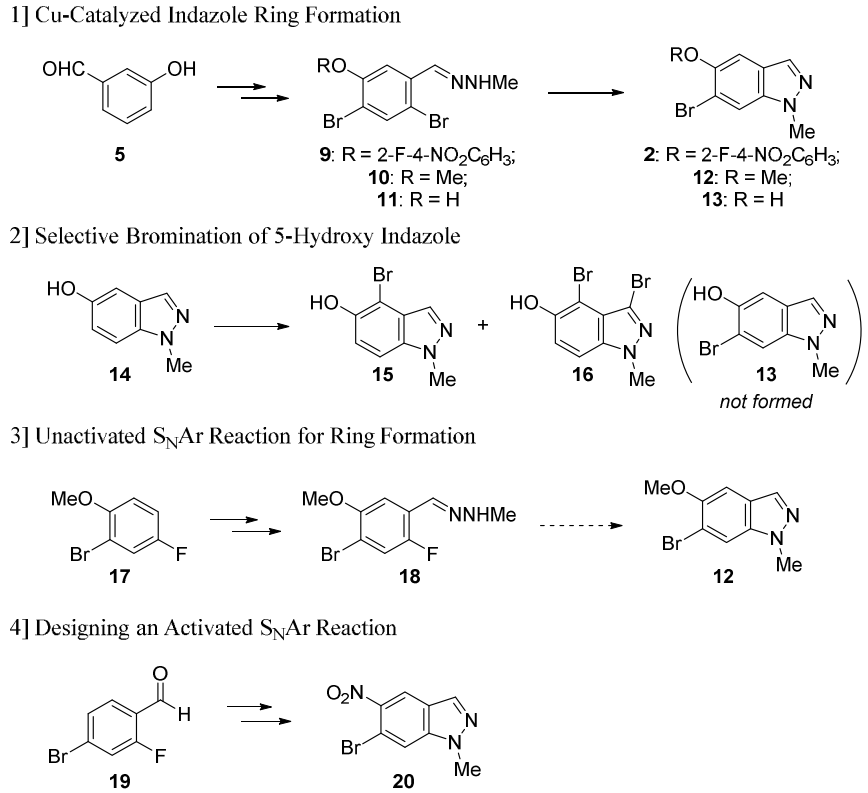

For the selective bromination investigation, methylindazole **14** was utilized since it is commercially available to some extent. Selective mono-bromination at C6 would provide a penultimate intermediate **13**. Although the most electrophilic site of **14** for halogenation appears to be C4 based on a literature example,[9] our plan was to incorporate dibromination followed by selective debromination, should monobromination prove unselective. Reaction of **14** with NBS in THF at 25 °C for 16 h provided **15** instead of the desired regioisomer **13**. Attempts at dibromination were also unsuccessful: when **15** was further reacted with NBS, 3,4-dibromoindazole **16** was obtained. A similar outcome was noted when NIS was substituted for NBS in the reaction with **14**. Since no useful C6 halogenation conditions were identified, all investigations utilizing **14** as a raw material were terminated.

2. Alternate Indazole Ring Formation through S_NAr Reaction. Based on our learnings surrounding the Cu-catalyzed indazole formation step, we focused on alternative means to close the indazole ring. One approach was to investigate an S_NAr reaction for the indazole ring forming step. To this point, such an approach had gone under-investigated because previous starting materials had an electronically deactivating ether or phenol functionality in the 5-position, such as compounds **9**, **10**, and **11**. In order to enable S_NAr reactivity in this system, it was determined that a strongly electron-withdrawing group in the C5-position was crucial. Furthermore, these intermediates present a bromine atom as the leaving group, which was also unfavorable for S_NAr reaction. A brief investigation of the S_NAr approach with the unactivated substrate **17** was undertaken. After formation of hydrazone **18**, all attempts at intramolecular S_NAr cyclization to the desired indazole **12** failed (Scheme 2, Equation 3).

In order to perturb the electronics of the aromatic ring, we decided to radically alter the synthetic approach. Readily available 4-bromo-2-fluorobenzaldehyde (**19**) was identified as a

logical starting point for the activated S_NAr investigation. With the bromide, aldehyde and fluoride in place, we focused on nitration at C5 in order to obtain the correct substitution pattern as well as to introduce S_NAr reactivity. Then, the nitro group in the product would serve as an activator for S_NAr reactions while acting as a masked phenol. It was envisioned that the chemistry needed to enable this synthetic approach would consist of: 1) Aromatic ring nitration; 2) S_NAr reaction to form indazole **20**; 3) Conversion of a nitroarene to phenol; and 4) Diaryl ether formation, which had already been demonstrated in a previous synthesis.

A. Aromatic Ring Nitration. Nitration of benzaldehyde **19** was initially performed as a conventional batch process with KNO_3 in concentrated H_2SO_4 to provide the nitrobenzene **21** according to a known literature method.[10] Although high yield and excellent regioselectivity were achieved for the isolated product (90% yield, >99.5% desired regioisomer), the portion-wise addition of KNO_3 to the solution of **19** in H_2SO_4 was noted to be strongly exothermic. Even with active cooling, at 100 g scale, an exotherm from 0 to 30 °C occurred in a span of <5 min, which gave us great concern for runaway potential. The exotherm was reduced by switching from KNO_3 to concentrated HNO_3 (65%, w/w). Upon controlled addition of HNO_3 to a solution of **19** in concentrated H_2SO_4 at 0 °C, the reaction demonstrated a subdued exotherm, and the internal temperature did not exceed 10 °C. Although differential scanning calorimetry (DSC) demonstrated the stability of isolated **21** was well maintained at temperatures up to 200 °C, further mitigation of the potential safety hazard from rapid heat evolution was deemed necessary, especially when considering scale-up.

Aromatic nitration in continuous flow has been demonstrated on both lab and production scale.[11] Here, continuous processing offers a significant safety benefit compared to batch mode.

Since this nitration was determined to be a rapid reaction, the necessary volume of a continuous flow reactor would be very small relative to a batch reactor. The small reactor dimensions would impart superior heat and mass transfer to the process, limiting the potential for thermal runaway, as well as minimizing the overall amount of material at risk, should a runaway occur. Therefore, nitration of **19** was investigated in continuous mode. For the continuous reaction, a mixture of HNO_3/H_2SO_4 was combined using a Tee-mixer with a premixed solution of **19** in H_2SO_4 and introduced into a plug flow reactor (PFR). The PFR (ID = 6 mm, length = 24 m) was constructed of Polytetrafluoroethylene (PTFE) and immersed in a cooling bath at 3 °C, but the temperature inside the reactor was not measured.[12] A calculated residence time (reactor volume / volumetric flow rate) of about 23 min in the PFR was sufficient to provide >98% reaction conversion (HPLC area%) with <2 HPLC area% of the undesired 3-nitro regioisomer. Although the level of the 3-nitro regioisomer was higher than the batch process (typically 0.3–0.8%), it was well rejected during the crystallization step and posed little impact in the downstream chemistry. The reactor outflow was collected and quenched by adding it to ice. Extraction with dichloromethane and solvent exchange into heptane afforded **21** as a crystalline solid in 88% yield. The majority of the product loss occurred during the extraction and crystallization, which are not yet optimized. It should be noted that the use of dichloromethane as extraction solvent was to enable rapid proof of concept and a study to replace it with a more sustainable solvent is ongoing. The continuous nitration process was demonstrated at 540 g scale, whereas the batch process was not developed beyond 100 g batch size. Overall, the nitration of **19** to afford **21** proved robust and versatile in that a batch or continuous process may be utilized for manufacturing. Given the equipment simplicity and inherent safety benefits of continuous flow nitration, the continuous process is currently in favor for further scale up.

B. Indazole Ring Formation via Hydrazone Formation and S_NAr Reactions. Following a literature procedure for preparation of 6-bromo-1-isopropyl-5-nitro-1*H*-indazole from **21** and isopropylhydrazine in *N*,*N*-dimethylformamide (DMF) at 150 °C for 5 h,[13] **21** was subjected to analogous reaction conditions (Table 1). Such a single pot transformation was desired, since it would avoid isolation of the hydrazone intermediate. Using methylhydrazine instead of isopropylhydrazine with a reaction time of 2 h in a pressurized autoclave, indazole **20** was obtained in good isolated yield (64%; Table 1, Entry 1). Optimization of the reaction parameters included screening of solvent and temperature in an effort to avoid the high temperature conditions. At lower temperature, the reaction was found to be complete after heating at 50 °C for 2 h (Table 1, Entry 2) to provide **20** in 70% yield. This result may indicate that the methylhydrazone intermediate **22** is more activated for the S_NAr than was the reported isopropylhydrazone.[13] Changing the reaction solvent from DMF to a mixture of EtOH/H_2O (5:1) caused slower cyclization, as a 40:52 ratio of the desired product **20** and hydrazone intermediate **22** was observed by HPLC at the end of reaction (Table 1, Entry 3). We postulated that a base additive would better facilitate the indazole formation by neutralizing the HF produced from cyclization and maintaining a high pH throughout the process. Additional rate acceleration may also be possible through deprotonation of the transient hydrazone intermediate, which may serve as a stronger nucleophile in the intramolecular nucleophilic substitution. Accordingly, addition of 1.5 equiv Et_3N with higher reaction temperature resulted in higher conversion (Table 1, Entry 4). Given that potassium carbonate (K_2CO_3) proved to be the optimal base for similar transformations,[14] it was applied to the formation of **20**. Indeed, addition of 1.5 equiv K_2CO_3 was found to promote the S_NAr reaction, providing **20** as the dominant product by HPLC (Table

1, Entry 5). Further optimization was realized by screening additional solvents (Table 1, Entries 6–9). An aqueous mixture of isopropanol (IPA) proved optimal as it gave the highest conversion rate and HPLC purity of the isolated product (Table 1, Entry 7). After the reaction was complete, addition of water and isolation of the resulting solid afforded **20** in 76% yield at 500 g scale (Table 1, Entry 10). It is noteworthy that no evidence of the isomeric 2*H*-indazole was observed using this synthetic approach.

Table 1. Solvent screen and additive effect on the synthesis of **20** from **21** and $MeNHNH_2$

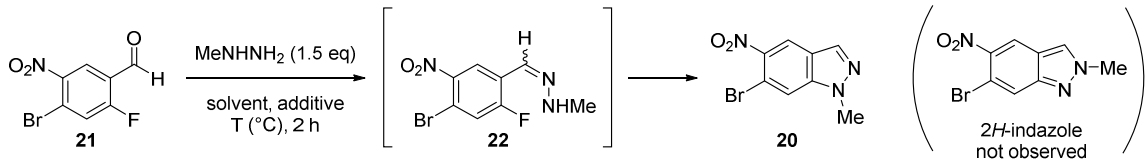

Entry	Scale (g)	Solvent	T (°C)	Additive (1.5 eq)	HPLC area% Ratio (20:22:others)
1[a]	300	DMF	150	none	ND
2[b]	5	DMF	50	none	ND
3	5	EtOH:H_2O (5:1)	50	none	40:52:8
4	2	EtOH:H_2O (2:1)	80	Et_3N	78:10:12
5	4	EtOH:H_2O (2:1)	80	K_2CO_3	85:3:12
6	5	MeOH:H_2O (2:1)	80	K_2CO_3	14:29:57
7	5	IPA:H_2O (2:1)	80	K_2CO_3	95:2:3
8	5	THF	80	K_2CO_3	95:0:5
9	5	2-MeTHF	80	K_2CO_3	80:3:17
10[c]	500	IPA:H_2O (2:1)	80	K_2CO_3	80:1:19

[a] reaction was conducted in autoclave, 64% isolated yield, 99.4% HPLC purity; [b] reaction was conducted in a round bottom flask, 70% isolated yield, 97.8% HPLC purity; [c] reaction time was 6 h, 76% isolated yield, 95.8% HPLC purity. ND = not determined.

C. Transformation of Nitroindazole to Aminoindazole. The nucleophilic displacement of a nitro group with an oxygen nucleophile has been achieved on nitroarenes bearing electron-withdrawing groups or halogens,[15] which we intended to adapt for nitroindazole **20**. We began this investigation by screening hydroxide, phenoxide, and methoxide with **20** in the hope of direct conversion of the nitro group to the corresponding phenol or ether. Unfortunately, direct functionalization of indazole **20** to the desired phenol or ether was unsuccessful; in all cases unreacted **20** was recovered.

Next, we turned our attention to a two-step process consisting of nitro reduction to aminoindazole **23** (Table 2) followed by hydrolysis of the amino functionality to hydroxylindazole **13** (Table 3). Three different nitro reduction methods were investigated for the conversion of **20** to **23**: 1) Bechamp type reaction with Fe/NH_4Cl;[16] 2) hydrazine or methylhydrazine with Raney nickel (Ra-Ni);[17] and 3) catalytic hydrogenolysis.[18] In the Bechamp method, Fe powder (4 equiv) was added to an EtOH/H_2O (3:2) solution containing NH_4Cl (10 equiv) at 90 °C for 2 h. After extractive work up with EtOAc, **23** was isolated in 81% yield as a crystalline solid. This method was not viewed favorably within current process development, as the heavy iron powder and excess NH_4Cl solid raised mixing and suspension concerns, as well as extra operational burden in the work-up and the handling of metal waste.

Hydrazines are known hydrogen donors in various hydrogenation reactions.[19] In the Raney nickel approach, hydrazine or methylhydrazine serves as the stoichiometric reductant in the presence of the nickel catalyst. This reaction could be performed either under hydrogen pressure or with an inert environment (Table 2, Entries 1–3). In all cases, the debrominated byproduct **24** was observed as an impurity. Although the initial results proved promising from a reactivity perspective, scale up of Ra-Ni reductions can prove challenging due to the difficulty of

suspending the dense metal catalyst. Additionally, a process safety assessment indicated a high level of concern with regards to the use of pyrophoric Raney nickel in combination with a hydrazine. Therefore, the decision was made to explore other reduction options for the conversion of **20** to **23**.

In the metal catalyzed hydrogenolysis approach (Table 2, Entries 4–8), our goal was to develop a batch reaction which could then potentially be converted to a continuous packed-bed transformation. In the batch process, while the reaction employing Raney nickel catalyst at 25 °C resulted in incomplete conversion, reaction of **20** with Pt/C catalyst (5% w/w metal loading on carbon, dry basis) in 5:1 EtOH/water at 25 °C provided a 6:1 ratio of desired product **23** and debrominated byproduct **24** (Table 2, Entries 4 and 5). When the catalyst was changed to sulfided Pt/C, reduced production of **24** was observed, but the reaction did not go to completion after 20 h at 60 °C (Table 2, Entry 6). Finally, by replacing EtOH/water with THF as the reaction solvent, the catalytic hydrogenation achieved completion with only a small amount of **24** generated. After filtration to remove the catalyst and concentration of the solvent, addition of EtOH/H_2O precipitated the product **23**, which was isolated in 83% yield with 98.6% HPLC purity on 283 g scale. With respect to these conditions, there were clear performance differences between the 5 g front run and the larger batch (Table 2, Entries 7 and 8). Further work must be done to understand the scale up parameters that will enable robust production.

In all three nitro reduction methods, debrominated by-product **24** was observed. Fortunately, **24** is largely purged during subsequent synthetic steps. The debrominated analog does not participate in the downstream Suzuki cross coupling and is simply purged during isolation of the cross-coupled product (>90% rejection at 1% w/w loading with respect to **2**). Nitroindazole **20** may be reduced to aniline **23** utilizing at least three different methods, any of

which could potentially be further developed into a commercial manufacturing process. We investigated all three methods in an attempt to provide flexibility for future manufactures. The ultimate selection of methodology will be based on a combination of process performance and the available equipment and technical expertise at the commercial manufacturing site.

Table 2. Preparation of aminoindazole **23**

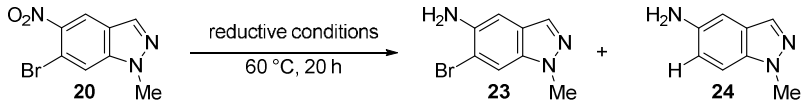

Entry	Scale (g)	Reductant	Catalyst (0.1 g/g)	Solvent	HPLC area% ratio (23:20:24)
1[a]	20	$NH_2NH_2•H_2O$ (2.5 eq) with H_2 (1 atm)	Ra-Ni	EtOH	93:0:6
2[b]	80	methylhydrazine (2.5 eq) with H_2 (1 atm)	Ra-Ni	EtOH	97:0:2
3	5	methylhydrazine (2.5 eq)	Ra-Ni	EtOH	85:6:5
4[c]	1.5	H_2 (1 atm)	Ra-Ni	EtOH:H_2O (5:1)	30:18:0
5[c]	2	H_2 (1 atm)	Pt/C	EtOH:H_2O (5:1)	78:0:12
6	5	H_2 (1 atm)	Pt(S)/C	EtOH:H_2O (5:1)	54:43:0.5
7	5	H_2 (1 atm)	Pt(S)/C	THF	98:0:0.5
8[d]	283	H_2 (1 atm)	Pt(S)/C	THF	90:3:3

[a] 79% isolated yield, 97% HPLC purity; [b] 76% isolated yield, 97% HPLC purity; [c] reaction at 25 °C; [d] Reaction was conducted for 10 h, 83% isolated yield, 98.6% HPLC purity.

Since methylhydrazine was used for the indazole formation, it could potentially serve as a hydrogen source in the subsequent nitro reduction. This approach would allow for a one-pot preparation of **23** from **21** using methylhydrazine and Raney nickel catalyst. In practice, after indazole formation using the conditions in Table 1, additional methyhydrazine was added to the reaction mixture, followed by Raney nickel catalyst. The first stage of the optimized process used K_2CO_3 (1.5 equiv) in IPA/H_2O with methylhydrazine (1.5 equiv) at 60 °C for 2 h. After

cooling the reaction mixture, the second stage was then initiated by addition of methylhydrazine and Raney nickel. After refluxing the reaction for 15 h, removal of the catalyst by filtration and cooling crystallization of the product from IPA/H_2O provided **23** in 60% yield (96% HPLC purity) from **21**.

D. Hydroxyindazole Formation from Aminoindazole Hydrolysis. The penultimate step to **2** involved hydrolysis of **23** to 5-hydroxyindazole **13**. Diazotization conditions[20] with $NaNO_2$ and H_2SO_4 or HCl resulted in formation of the corresponding diazonium intermediate as evidenced by LCMS, which showed complete conversion to the diazonium salt of **23** ($[M]^+$ m/z = 237/239). Despite extensive efforts, the diazonium intermediate did not undergo the desired hydrolysis step. When higher temperatures were applied to the hydrolysis attempts, multiple unidentified byproducts were observed, likely due to several decomposition pathways of the diazonium intermediate.

Since aqueous H_3PO_4 at high temperature has been reported for the hydrolysis of aniline to phenol,[21] it was investigated for the hydrolysis of **23** (Table 3). Initially, a solution of **23** in 5:1 v/v of 85% w/w aq. H_3PO_4/H_2O was refluxed at 135 °C for 40 h. We were pleased when these conditions afforded 71% conversion of **23** to **13** (Table 3, Entry 1). A 144 h (6 days) reaction time delivered 98% conversion (Table 3, Entry 2). However, the long hold at high temperature required to achieve high reaction conversion was deemed impractical. In order to achieve higher temperatures under pressure, screening reactions were conducted in sealed glass tubes. While it required 11 h at 160 °C to reach 80% of **13** with 18% unreacted aminoindazole **23** by HPLC area%, reaction at 200 °C gave 92% of **13** with only 2% of **23** remained after 1 h reaction time (Table 3, Entries 3 and 4). Guided by process safety considerations under extreme

conditions (acidic conditions at high temperature and pressure), continuous processing in a PFR was investigated. Proof of concept for the continuous reaction was achieved using a Hastelloy® type B-2 PFR with pressurization to 83 psig (pound-per-square-inch, gauge): a 1 h nominal residence time (reactor volume / volumetric flow rate) at 200 °C produced 130 g of **13** in 71% isolated yield (Table 3, Entry 5). However, after completion of a flow process lasting about 16 h, contamination of the collected reaction mixture with nickel (Ni is a major component of Hastelloy® type B-2) was noted by Inductively Coupled Plasma Mass Spectrometry (ICP-MS) analysis, indicating corrosion of the Hastelloy® coil. Although it did not ultimately affect the quality of isolated **13** or the indazole **2** in the subsequent step, extreme caution is merited in this instance, as reactor rupture would occur upon extended exposure and it is not recommended that this process be run in Hastelloy®. Inherently unsafe operations such as this are not conducted as a general practice at Eli Lilly. A corrosion study of different materials to hopefully identify a more suitable PFR material of construction revealed a 0.35% w/w loss for a Hastelloy® coupon in the mixture of H_3PO_4/H_2O after 4 days at 160 °C, while a tantalum coupon showed 0.015% w/w loss under identical conditions. No weight loss or visible physical change (e.g., softening, coloring, cracking) was observed for PFA (perfluoroalkoxy) coupon under the same conditions. Therefore, hydrolysis of **23** was next accomplished using a stainless steel encompassed PFA PFR on lab scale (5 g) at 160 °C with a residence time of 10 h, affording **13** in 77% isolated yield with 97% HPLC purity. In this case, 160 °C was selected due to concern over softening of the PFA tubing at higher temperatures. Backpressure was applied (70 psig), as Aspen prediction indicates 33 psig of pressure is required to prevent vaporization of the reactor contents. Overall, the conversion from **23** to **13** in H_3PO_4/H_2O under thermal conditions is a relatively clean reaction, as only the starting material and desired product are observed as the major components

(generally >93% HPLC area combined, as shown in Table 3) when monitoring by HPLC. Neutralization of the acidic reaction mixture with base and extraction into EtOAc provided good recovery of isolated product (Table 3, Entry 1). The more operationally straightforward precipitation method from diluted reaction mixture gave less efficient recovery of product due to material loss in aqueous solution (Table 3, Entries 5 and 6).

Table 3. Reaction conditions for conversion of aminoindazole **23** to hydroxyindazole **13**

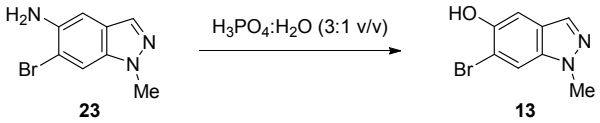

Entry	Scale (g)	Temp (°C)	Time (h)	Reactor	HPLC area% ratio (13:23:others)	Isolated Yield (HPLC area%)
1[a]	1	135	40	RBF, condenser	71:27:2	70% (99%)
2	20	135	144	RBF, condenser	95:2:3	ND (ND)
3	0.5	160	11	Sealed glass tube	80:18:2	ND (ND)
4	2	200	1	Sealed glass tube	92:2:6	60% (92%)
5	182	200	*ca.* 1[b]	Hastelloy® PFR	81:5:14	71%[c] (94%)
6	5	160	10[b]	PFA PFR	89:4:7	77%[c] (97%)

[a] H_3PO_4:H_2O (5:1, v/v); [b] nominal residence time of flow reaction; [c] ~13% product loss in aq. solution during work-up. RBF = Round Bottom Flask, ND = Not Determined.

Additional screening of the H_3PO_4 : H_2O ratio (from 6:1 to 1:6, v/v) indicated an optimal operational range of 2–3:1 H_3PO_4:H_2O (or 65–71% w/w solvent H_3PO_4 strength) in order to achieve the highest reaction conversion at 160 °C within 5 h (Figure 3). Further investigation and scale-up of this reaction conditions is currently ongoing and will be reported in due course.

Figure 3. Reaction screening for optimal solvent H_3PO_4 strength[a]

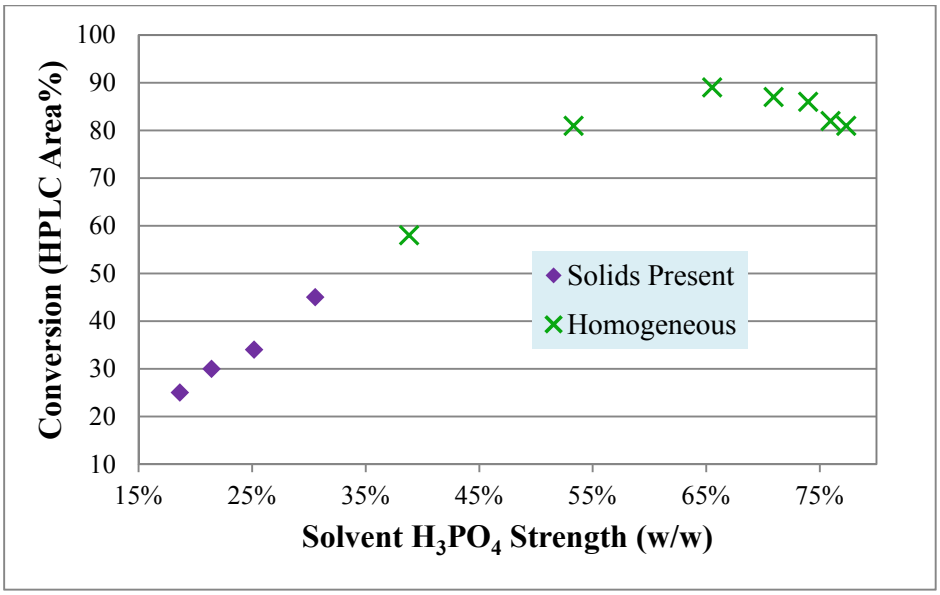

[a] Reactions were conducted in a mixture of H_3PO_4 and H_2O (12 mL per gram of **23**) and stopped after stirring for 5 h at 160 °C.

E. Preparation of 2. We have previously disclosed a method for similar diaryl ether formation.[6a] The key challenge to the success of this approach is in formation of an appropriate phenolic coupling partner. The newly-developed route benefits in that **13** has the isomerically pure methylated indazole ring fully formed and no further manipulations are necessary after the S_NAr ether formation with fluoride **7**. Therefore, the aryl ether formation conditions required little effort for optimization in terms of a base, solvent, temperature and reaction rate. The optimized conditions used K_2CO_3 as base, with THF as solvent at 55 °C for 14 h to give >90% assay yield of **2**. After aqueous work-up, crystallization from toluene afforded 72% yield of purified **2** (Scheme 3).

Scheme 3. Developed alternative synthesis of indazole aryl ether **2**

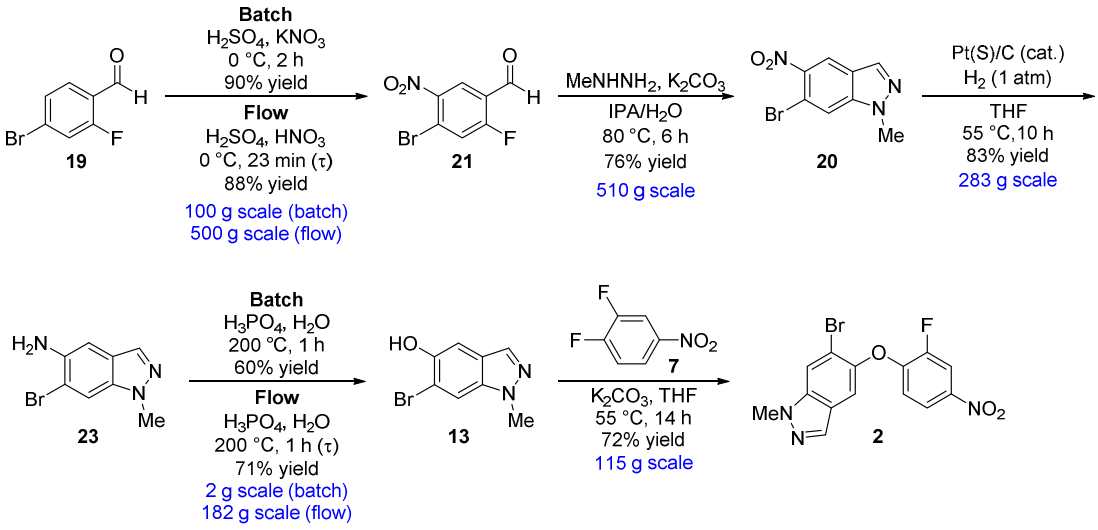

Figure 4 shows an HPLC chromatogram of indazole **2** derived from the new route ("nitro route") compared with crude and recrystallized material from the Ullmann route. The overall impurity load from the new method is significantly reduced versus the Ullmann method both in terms of overall number of impurities as well as area% of individual species. Although the impurities from the Ullmann route are ultimately purged to acceptable levels in the downstream steps, the new synthesis is viewed as advantageous given the greatly improved purity profile for this proposed regulatory starting material (**2**). Given that **2** contains a genotoxic alerting functionality (aromatic nitro), it is not surprising that impurities related to **2** would likely also be of similar concern. We have in fact identified several such impurities derived from the Ullmann route and have characterized their downstream behavior in order to understand their fate as well as demonstrate purge to acceptable limits. Since the new method has fewer overall such impurities, this task is greatly simplified should long term manufacturing utilize the new route. Finally, shown in Figure 5 are photographs of typical material derived from the Ullmann route compared to that from the new route. While the color from **2** has been shown to normally purge in downstream operations, there have been individual developmental batches of **2** that have resulted in colored intermediates and API.

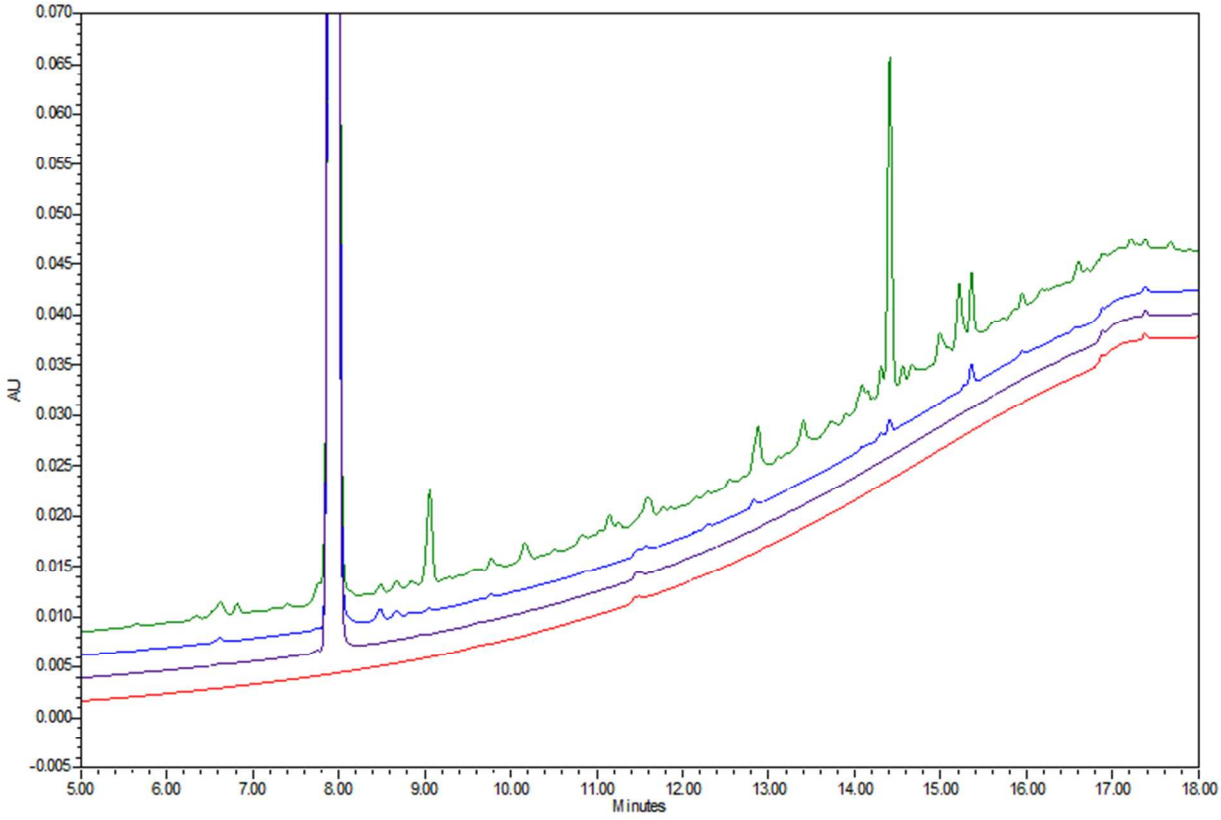

Figure 4. Comparison of compound **2** productions by HPLC analysis (Trace identification from top to bottom: Green = Ullmann route crude solids, Blue = Ullmann route recrystallized solids, Purple = nitro route solids, Red = blank injection).

Figure 5. Comparison of compound **2** productions by color (**A**. Sample of **2** from Ullmann route; **B**. Sample of **2** from nitro route).

CONCLUSION

An alternative indazole synthesis for merestinib starting material **2** has been developed. Indazole **2** is common to multiple existing merestinib syntheses, and the new method of preparation offers multiple advantages over previous methods. The key transformation in the new preparation of **2** is an intramolecular S_NAr reaction to form the indazole heterocycle; this reaction ensures that the methyl group is installed in a selective manner. The intramolecular S_NAr precursor is derived from a readily available aldehyde building block and the cyclization itself is enabled by use of an excellent S_NAr leaving group (fluoride) and the strongly electron-withdrawing nitro group *para* to the fluorine. These two factors appear to be necessary for the success of this transformation, as less activated systems didn't successfully yield product. We chose to develop the nitration using continuous flow methodology and showed that the reaction could be run using a small PFR, which has several safety benefits. The new synthesis avoids the need for any tedious clean-up procedures such as metal scavenging during manufacturing. The most significant challenge during the development was identification of suitable conditions to convert the nitro group into the phenolic functionality. Ultimately, nitro reduction to the aniline followed by a high temperature acidic hydrolysis enabled by continuous processing allowed for a successful transformation. The synthesis of **2** was completed by diaryl ether formation, which relied on conditions modified from a previously reported approach. Although the new synthesis route is one step longer than the Ullmann route, it is believed that the new route will prove to be more robust in terms of process performance and yield than the problematic Ullmann cyclization. Additionally, indazole **2** derived from the new route is superior to that from the Ullmann route in terms of impurity profile and color.

EXPERIMENTAL SECTION

General Information

All commercially available chemicals and solvents were used directly as received. Melting points were recorded (uncorrected) on a Buchi M-565 melting point monitor. ^{1}H NMR spectra were recorded on Bruker AV 300 and 400 MHz spectrometer. ^{13}C NMR spectrum were recorded using the same spectrometers at 75 and 100 MHz, respectively. Chemical shifts are reported in parts per million (δ), coupling constants (*J*-values) are reported in hertz (Hz), and spin multiplicities are indicated by the following symbols: s (singlet), d (doublet), t (triplet), q (quartet), m (multiplet), bs (broad singlet). Mass spectra were obtained from Agilent 1290 Infinity II with 6130 Chemstation and Agilent 1200 Infinity II with 6130 Chemstation. GCMS were recorded using Agilent technologies; 7890B GC with 5977B MS. Infrared spectra were obtained on a PerkinElmer Spectrometry.

Reactions were monitored by TLC (Thin Layer Chromatography), or reverse-phase HPLC using an Atlantis d-C18 4.6 mm × 250mm column with 5 μm particle size. For HPLC: Solvent A was a 0.1% solution of TFA in water; Solvent B was MeOH. The flow rate was 1.0 mL/min with a column temperature of 40 °C. Detection wavelength: 210 nm. The HPLC gradient method is shown below:

Time/min	Solvent A %	Solvent B%
0	70	30
15	5	95
18	5	95
18.1	70	30
20	70	30

4-Bromo-2-fluoro-5-nitrobenzaldehyde (21) (batch reaction): To a stirred solution of 4-bromo-2-fluorobenzaldehyde **19** (100 g, 493 mmol) in conc. H_2SO_4 (500 mL) at 0 °C (ice-water bath) was added KNO_3 (54.3 g, 547 mmol) portion-wise [*CAUTION*: exothermic; internal temperature increased to 30 °C]. The mixture was stirred at 0 °C for 2 h, at which time TLC (heptane:acetone = 2:1, UV) indicated completion of the reaction. The reaction mixture was slowly poured into 5 kg of crushed ice with stirring. The solid thus precipitated was filtered, washed with water (3 × 500 mL), and dried to afford **21** (110 g, 90% yield) as an off-white solid. m.p.: 46.4 – 48.5 °C; IR (thin film, cm^{-1}) 3102, 3050, 2882, 1700, 1604, 1571, 1532, 1459, 657, 605; ^{1}H NMR (400 MHz, DMSO-d_6): δ 10.14 (s, 1H), 8.50 (d, J_{H-F} = 6.4 Hz, 1H), 8.22 (d, J_{H-F} = 10.0 Hz, 1H); ^{13}C NMR (DMSO-d_6, 75 MHz): δ 186.4, 163.39 (d, J_{CF} = 266.7 Hz), 146.9, 127.1, 124.3, 124.1, 121.6; HPLC t_R = 10.7 min (210 nm); GCMS: calculated for $C_7H_3BrFNO_3$ 246.9, found 246.9.

4-Bromo-2-fluoro-5-nitrobenzaldehyde (21) (flow reaction): PFR: PTFE tubing, ID = 6 mm, length = 24 m, maintained at 3 °C in ice bath. Feed solution A: 4-bromo-2-fluorobenzaldehyde (0.50 kg, 2.46 mol) in H_2SO_4 (1.84 kg). Feed solution B: HNO_3 (65% w/w, 0.36 kg, 3.69 mol) in H_2SO_4 (2.76 kg). At first, CH_2Cl_2 was pumped into the PFR with Pump A and Pump B (both are piston pumps made of PTFE) to achieve a steady state of the corresponding flow rates (Pump A rate = 9.2 g/min; Pump B rate = 12.2 g/min), which is adjusted by weight loss of two CH_2Cl_2 feed solutions and reflects a theoretical 1.5 equiv. of HNO_3 in relative to the aldehyde starting material. After the PFR was filled with CH_2Cl_2, and confirming normal operation for 30 min, the pumps were stopped. Feed solutions A and B were then pumped into the PFR by Pumps A and B respectively with the temperature of the reactor maintained at 3 °C. The mass flow rates

were monitored such that 9.2 g/min was delivered from Pump A and 12.2 g/min from Pump B. These conditions resulted in a nominal residence time of 23 min. The reactor outflow was collected in a receiving reactor maintained at 3 °C. After the feed solutions were consumed, conc. H_2SO_4 (0.92 kg) was pumped into the PFR to push out the reaction mixture, followed by CH_2Cl_2 until colorless liquid was observed at the reactor outlet. The collected mixture was then poured onto cracked ice (7.5 kg) slowly. The mixture was extracted with CH_2Cl_2 (3 × 2.5 L). The combined organic phase was washed with 10% aqueous K_2CO_3 solution (2 × 2.5 L) to adjust the pH to ≥7, washed with H_2O (2.5 L) and concentrated under reduced pressure. Heptane (1.5 L) was added and the resulting mixture was stirred for 1 h and then cooled to 2 °C, held for 50 min. A solid precipitated, which was collected by filtration and rinsed with heptane (0.5 L). The solid was dried under nitrogen at 23 °C to afford **21** (0.54 kg, 88% yield) as a yellow solid.

6-bromo-1-methyl-5-nitro-1*H*-indazole (20): To a 10 L jacketed reactor charged with aldehyde **21** (0.51 kg, 2.05 mol), isopropanol (1.53 L) and H_2O (0.765 L) at 24 °C was added K_2CO_3 (0.425 kg, 3.08 mol) in portions. After the suspension was warmed to 41 °C, methylhydrazine (0.142 kg, 3.08 mol) was added dropwise over 1 h. The reaction mixture was stirred for 1 h at 41 °C and then heated to 77 °C for 6 h and monitored by HPLC until the reaction was complete. The reaction mixture was cooled to 30 °C, water (5.1 L) was added into reaction mixture over 1 h, and the mixture was stirred at 15 °C. After stirring for 1.5 hours, the solid was collected by filtration, the wet cake was rinsed with water (1.02 L) and the solids were dried under nitrogen at 23 °C to provide **20** as a yellow solid (0.40 kg, 76% yield). m.p.: 161.9 – 165.9 °C; IR (thin film, cm^{-1}): 3104, 3067, 3027, 2952, 1686, 1608, 1566, 1515, 1487, 655, 623; ^{1}H NMR (400 MHz, DMSO-d_6): δ 8.61 (s, 1H), 8.33 (s, 2H), 4.11 (s, 3H); ^{13}C NMR (DMSO-d_6, 75 MHz): δ 143.6,

140.5, 135.6, 121.7, 120.4, 116.2, 110.7, 36.4; HPLC t_R = 12.4 min (210 nm); GCMS: calculated for $C_8H_6BrN_3O_2$ 255.0, found 255.0.

6-bromo-1-methyl-1*H*-indazol-5-amine (**23)**: To a 10 L 4-necked round bottom flask charged with a solution of **20** (0.283 kg, 1.11 mol) in THF (3.0 L) at 23 °C was added Pt(S)/C (5% w/w metal loading on carbon, dry basis; 0.03 kg, 7.7 mmol) in one portion. The reaction mixture was purged with nitrogen (5×), and then purged with hydrogen (3×) at atmospheric pressure. The mixture was heated to 60 °C and stirred under hydrogen for 10 h, at which time HPLC analysis indicated completion of the reaction. The reaction mixture was cooled to 25 °C, and THF (3.0 L) was added. After stirring for 1 hour, the mixture was filtered through Celite® (128 g) to remove the catalyst, and the filtrate was concentrated to 0.4 L. To the residue was added a mixture of EtOH (0.32 L) and H_2O (3.0 L) slowly with stirring. A solid formed and was stirred for 1 h and then collected by filtration. The solid was dried under nitrogen at 24 °C to afford **23** (0.21 kg, 83% yield) as a brown solid. m.p.: 153.6 – 159.2 °C; IR (thin film, cm^{-1}) 3415, 3304, 3206, 3090, 2940, 1677, 1624, 1563, 975, 868, 841, 621; ^{1}H NMR (400 MHz, DMSO-d_6): δ 7.85 (s, 1H), 7.77 (s, 1H), 7.04 (s, 1H), 4.95 (bs, 2H), 3.93 (s, 3H); ^{13}C NMR (DMSO-d_6, 100 MHz): δ 139.8, 135.2, 130.9, 124.5, 113.4, 112.7, 102.8, 35.9; HPLC t_R = 5.7 min (210 nm); LCMS: $[M+H]^+$: calculated for $C_8H_9BrN_3$ 226.0, found 225.8.

6-bromo-1-methyl-1*H*-indazol-5-amine (23) (one-pot procedure from aldehyde 21 with MeNHNH$_2$/Raney-Ni): A 4-necked round bottom flask equipped with a mechanical stirrer and thermocouple was charged with aldehyde **21** (10.0 g, 40.3 mmol), K_2CO_3 (8.35 g, 60.5 mmol), isopropanol (30 mL) and H_2O (15 mL) at 25 °C. 1-Methylhydazine (2.76 g, 60.5 mmol) was

added dropwise at 25 °C. The reaction mixture was heated to 80 °C and stirred for 2 h, at which time LCMS showed completed conversion to indazole **20**. After the reaction was cooled to 25 °C, Raney-Ni (2.0 g, 50% w/w in aq. solution, 17.8 mmol) was added along with additional 1-methylhydazine (1.84 g, 40.3 mmol) and the mixture was heated to reflux for 20 h. After cooling and addition of THF (100 mL), the mixture was filtered through Celite® (20 g), and the residue was concentrated to remove the organic solvents. The solid was dissolved in MTBE (50 mL) and then acidified to pH = 2 with 1 N HCl. The separated aqueous product solution was washed with MTBE and then basified with 30% aq. NaOH solution to pH = 8–9. The resulting suspension was stirred and solid was collected by filtration. The solid was washed with water (2 × 50 mL) and dried under vacuum to provide **23** (5.5 g, 60% yield) as a brown solid.

6-bromo-1-methyl-1*H*-indazol-5-ol (13) (batch reaction): To a stirred suspension of **23** (2.00 g, 8.9 mmol) in water (6 mL) in a glass tube, phosphoric acid (85% in water, 18 mL) was added at 25 °C. The tube was sealed and heated to 200 °C for 1 h. After completion of the reaction (monitored by TLC & LCMS), the reaction mixture was cooled to 25 °C and poured into crushed ice (300 g) with stirring. The solid thus precipitated was filtered, washed with water (3 × 30 mL) and dried to afford **13** (1.22 g, 60% yield) as a yellow solid. m.p.: 184.3 – 185.7 °C; IR (thin film, cm^{-1}) 3110, 2946, 1671, 1624, 1563, 1495, 627, 587 ; ^{1}H NMR (400 MHz, DMSO-d_6) δ 9.93 (bs, 1H), 7.93 (s, 1H), 7.86 (s, 1H), 7.17 (s, 1H), 3.97 (s, 3H); ^{13}C NMR (DMSO-d_6, 75 MHz): δ 148.2, 135.7, 131.5, 123.9, 114.0, 112.9, 103.9, 35.9; HPLC t_R = 9.2 min (210 nm); LCMS: $[M+H]^+$: calculated for $C_8H_8BrN_2O$ 227.0/229.0, found 227.0/228.9.

6-bromo-1-methyl-1*H*-indazol-5-ol (13) (flow reactor run): Two identical PFRs were constructed from Hastelloy® (B-2) tubing, ID = 6 mm, length = 32 m. One of the PFR was heated to 200 °C using high temperature oil bath. The second PFR was maintained at 7 °C for the reactor outflow. Feed solution A: a mixture of **23** (0.182 kg, 0.805 mol), water (0.60 L) and 85% w/w aq. H_3PO_4 (1.82 L) was heated to 51 °C and stirred until the solid dissolved completely. The mixture was cooled to 20 °C and was ready for use. Feed solution B: a solution of 85% w/w aq. H_3PO_4/H_2O (3:1, v/v). The outflow receiving flask consisted of a 20 L four-necked round bottom flask containing H_2O (9.1 L) cooled to 4 °C. Solution B was pumped into the PFR at 4.0 g/min for 30 min. Then, the flow of Solution B was stopped and the flow of Solution A was initiated into the PFR at 4.0 g/min. The flow rate was monitored by matching the actual weight loss of the feed solution with the calculated theoretical weight loss. The reactor outflow passed through the cooling coil and flowed into the receiving flask after 60 min residence time (not corrected for thermal expansion). After Solution A was fully consumed, Solution B was pumped into the system to push out the reaction mixture until colorless liquid was observed at the outlet. The collected mixture was stirred in the receiving flask at 5 °C for 1.5 h, and the precipitated solid was filtered and rinsed with H_2O (0.91 L). The solid was dried under nitrogen at 25 °C to afford **13** (130 g, 71% yield) as a dark brown solid.

Preparation of 6-bromo-5-(2-fluoro-4-nitrophenoxy)-1-methyl-1*H*-indazole (2): To a 2 L four-necked round bottom flask charged with **13** (0.115 kg, 0.51 mol) and THF (0.55 L) at 25 °C was added K_2CO_3 (0.77 kg, 0.55 mol) and 3,4-difluoronitrobenzene (0.83 kg, 0.52 mol). The resulting mixture was stirred at 55 °C for 14 h and then concentrated to 2–3 vol (<345 mL). Water (1.15 L) was slowly added, and the resulting solid was collected through filtration, rinsed

with H_2O (0.22 L), followed by EtOH (1.1 L). The yellow solid was dissolved in toluene (1.1 L) at 80 °C, to which activated carbon (57 g) was added. The resulting suspension was stirred at 80 °C for 5 h and the activated carbon was removed by filtration. After concentration to 2–3 vol, the mixture was stirred at 85 °C for 3 h and was cooled to 5 °C slowly. The suspension was stirred at 5 °C for 2 h. The solid was collected by filtration, rinsed with EtOH (0.22 L), and dried under nitrogen at 25 °C to afford **2** as a white solid (0.134 kg, 72% yield). m.p.: 182.2 – 187.5 °C; IR (thin film, cm^{-1}) 3044, 1675, 1601, 1521, 1484, 1431, 1405, 668, 623; ^{1}H NMR (400 MHz, DMSO-d_6) δ 8.36 (dd, J = 11.1, 2.8 Hz, 1H), 8.30 (s, 1H), 8.10 (s, 1H), 8.04–8.01 (m, 1H), 7.85 (s, 1H), 6.89 (t, J = 8.8 Hz, 1H), 4.09 (s, 3H); ^{13}C NMR (DMSO-d_6, 75 MHz): δ 152.6, 151.7, 151.6, 149.3, 144.0, 142.5, 142.4, 138.6, 133.3, 123.5. 121.8 (2C), 117.1, 115.6, 114.6, 114.1, 113.7, 113.4, 36.3; HPLC t_R = 15.5 min (210 nm); GCMS: calculated for $C_{14}H_9BrFN_3O_3$ 365.0/367.0, found 365.0/366.9. ^{1}H and ^{13}C NMR spectra are in agreement with those reported in literature.[6a]

ASSOCIATED CONTENT

Supporting Information

Schematic drawings of equipment set for Step 1 and Step 4 in PFR, as well as ^{1}H and ^{13}C NMR spectra for the compounds **2**, **13**, **20**, **21**, **23**. This material is available free of charge via the Internet at http://pubs.acs.org.

AUTHOR INFORMATION

Corresponding Author

*Email: ylu@lilly.com

Present Addresses

†Retired from Eli Lilly and Company.

Author Contributions

The manuscript was written through contributions of all authors. All authors have given approval to the final version of the manuscript.

Funding Sources

None.

ACKNOWLEDGEMENTS

We thank Dr. Martin Johnson for his suggestions concerning the continuous processing equipment sets and Mr. Richard Miller for running some of the experiments. Aileen Chapman provided valuable assistance in preparing the HPLC chromatograms. Jennifer Groh assisted with equipment drawings. We also thank Wenying Bi and Pingzhong Huang from Asymchem L.L.C. for their contributions.

REFERENCES

1) Liu, X.; Newton, R. C.; Scherle, P. A. *Expert Opin. Invest. Drugs* **2011**, *20*, 1225–1241.

2) (a) Li, T.; Pobanz, M. A.; Shih, C.; Wu, Z.; Yang, W. J.; Zhong, B. Preparation of amidophenoxyindazoles as inhibitors of c-MET. US 8030302 B2 20111004 and WO 2010011538 A1 20100128; (b) Yan, S. B.; Peek, V. L.; Ajamie, R.; Buchanan, S. G.; Graff, J. R.; Heidler, S. A.; Hui, Y.; Huss, K. L.; Konicek, B. W.; Manro, J. R.; Shih, C.; Stewart, J. A.;

Stewart, T. R.; Stout, S. L.; Uhlik, M. T.; Um, S. L.; Wang, Y.; Wu, W.; Yan, L.; Yang, W. J.; Zhong, B.; Walgren, R. A. *Invest. New Drugs* **2013**, *31*, 833–844.

3) Forde, P.M.; Rudin, C.M. *Expert Opin. Pharmacother.* **2012***, 13,* 1195–1201.

4) Yakes, F. M.; Chen, J.; Tan, J.; Yamaguchi, K.; Shi, Y.; Yu, P.; Qian, F.; Chu, F.; Bentzien, F.; Cancilla, B.; Orf, J.; You, A.; Laird, A. D.; Engst, S.; Lee, L.; Lesch, J.; Chou, Y.-C.; Joly, A. H. *Molecular cancer therapeutics* **2011**, *10*, 2298–2308.

5) (a) Devarakonda, S.; Ganesh, B.; Mann, J.; Govindan, R. *Expert Opinion on Orphan Drugs* **2015**, *3*, 1209–1218; (b) Gruellich, C. *Recent Results in Cancer Research* **2014**, *201*, 207–214.

6) (a) Kallman, N. J.; Liu, C.; Yates, M. H.; Linder, R. J.; Ruble, J. C.; Kogut, E. F.; Patterson, L. E.; Laird, D. L. T.; Hansen, M. M. *Org. Process Res. Dev.* **2014**, *18*, 501–510; (b) Frederick, M. O.; Calvin, J. R.; Cope, R. F.; LeTourneau, M. E.; Lorenz, K. T.; Johnson, M. D.; Maloney, T. D.; Pu, Y. J.; Miller, R. D.; Cziesla, L. E. *Org. Process Res. Dev.* **2015**, *19*, 1411–1417; (c) Cole, K. P.; Campbell, B. M.; Forst, M. B.; Groh, J. M.; Hess, M.; Johnson, M. D.; Miller, R. D.; Mitchell, D.; Polster, C. S.; Reizman, B. J.; Rosemeyer, M. *Org. Process Res. Dev.* **2016**, *20*, 820–830.

7) (a) Vina, D.; del Olmo, E.; Lopez-Perez, J. L.; Feliciano, A. S. *Org. Lett.* **2007**, *9*, 525–528; (b) Xiong, X.; Jiang, Y.; Ma, D. *Org. Lett.* **2012**, *14*, 2552–2555.

8) (a) Lebedev, A. Y.; Khartulyari, A. S.; Voskoboynikov, A. Z. *J. Org. Chem.* **2005**, 70, 596–602. (b) Pabba, C.; Wang, H.; Mulligan, S. R.; Chen, Z.; Stark, T. M.; Gregg, B. T. *Tetrahedron Lett.* **2005**, *46*, 7553–7557. (c) Duncan, N. C.; Garner, C. M. *Tetrahedron Lett.* **2011**, *52*, 5214–

5216. (d) Dong, C.; Xie, L.; Mou, X.; Zhong, Y.; Su, W. *Org. Biomol. Chem*. **2010**, *8*, 4827–4830.

9) Cheruvallath, Z.; Gwaltney, S. L.; Jennings, A. J.; Sabat, M.; Stafford, J. A.; Tang, M.; Wang, H. PCT Int. Appl. WO2009/140624 A2.

10) Kusakabe, K.; Ide, N.; Daigo, Y.; Tachibana, Y.; Itoh, T.; Yamamoto, T.; Hashizume, H.; Hato, Y.; Higashino, K.; Okano, Y.; Sato, Y.; Inoue, M.; Iguchi, M.; Kanazawa, T.; Ishioka, Y.; Dohi, K.; Kido, Y.; Sakamoto, S.; Yasuo, K.; Maeda, M.; Higaki, M.; Ueda, K.; Yoshizawa, H.; Baba, Y.; Shiota, T.; Murai, H.; Nakamura, Y. *J. Med. Chem.* **2013**, *56*, 4343–4356.

11) (a) Gage, J. R.; Guo, X.; Tao, J.; Zheng, C. *Org. Process Res. Dev.* **2012**, *16*, 930–933. (b) Kulkarni, A. A. *Beilstein J. Org. Chem*. **2014**, 10, 405–424. (c) Sharma, Y.; Joshi, R. A.; Kulkarni, A. A. *Org. Process Res. Dev.* **2015**, *19*, 1138–1147.

12) For the schematic drawing of equipment set for Step 1 in PFR, see Supporting Information.

13) Huang, L.; Liu, Y.; Li, T.; Huang, J.; Zhu, X. *Faming Zhuanli Shenqing* (2015), CN 104447765 A Mar 25, 2015.

14) Thomé, I.; Besson, C.; Kleine, T.; Bolm C. *Angew. Chem. Int. Ed.* **2013**, *52*, 7509–7513.

15) (a) Sarkate, A. P.; Bahekar, S. S.; Wadhai, V. M.; Ghandge, G. N.; Wakte, P. S.; Shinde, D. B. *Synlett.* **2013**, *24*, 1513–1516. (b) Zilberman, J. *Org. Process Res. Dev*. **2003**, *7*, 303–305 (c) Knudsen, R. D.; Snyder, H. R. *J. Org. Chem*. **1974**, *39*, 3343–3346.

16) Béchamp, A. *Annales de chimie et de physique*. **1854**, 42, 186–196.

17) Dull, G. M.; Wagner, J. M.; Caldwell, W. S.; Miller, C. H.; Schmitt, J. D.; Bhatti, B. S.; Hadimani, S. B. U.S. Patent, US 6337351 B1 2002.

18) (a) Wu, G.; Huang, M.; Richards, M.; Poirier, M.; Wen, X.; Draper, R. W. *Synthesis* **2003**, 1657–1660. (b) Blaser, H.; Steiner, H.; Studer, M. *ChemCatChem* **2009**, *1*, 210–221.

19) Crawford, J. J.; Ortwine, D. F.; Wei, B.; Young, W. B. PCT Int. Appl. (2013), WO 2013067274 A1.

20) (a) Vernekar, S. K. V.; Hallaq, H. Y.; Clarkson, G.; Thompson, A. J.; Silvestri, L.; Lummis, S. C. R.; Lochner, M. *J. Med. Chem.* **2010**, *53*, 2324–2328. (b) Shimada, I.; Maeno, K.; Kazuta, K.; Kubota, H.; Kimizuka, T.; Kimura, Y.; Hatanaka, K.; Naitou, Y.; Wanibuchi, F.; Sakamoto, S.; Tsukamoto, S. *Biorg. Med. Chem*. **2008**, *16*, 1966–1982. (c) Johnson, F.; Panella, J. P.; Carlson, A. A.; Hunneman, D. H. *J. Org. Chem*. **1962**, *27*, 2473–2478.

21) (a) Boyarskiy, V. P.; Belov, V. N.; Medda, R.; Hein, B.; Bossi, M.; Hell, S. W. *Chem. Eur. J.* **2008**, *14*, 1784–1792; (b) Li, J.; Kung, D. W.; Griffith, D. A. *Tetrahedron Lett.* **2010**, *51*, 3876–3878; (c) Lamberth, C.; Kessabi, F. M.; Beaudegnies, R.; Quaranta, L.; Trah, S.; Berthon, G.; Cederbaum, F.; Vettiger, T.; Prasanna, C. S. *Synlett*, **2014**, *25*, 858–856.